

Neurotransmitter selection by monoamine oxidase isoforms, dissected in terms of functional groups by mixed double mutant cycles

HUDSPITH, Lewis, SHMAM, Faraj, DALTON, Caroline F, PRINCIVALLE, Alessandra and TUREGA, Simon <<http://orcid.org/0000-0003-1044-5882>>

Available from Sheffield Hallam University Research Archive (SHURA) at:

<http://shura.shu.ac.uk/25186/>

This document is the author deposited version. You are advised to consult the publisher's version if you wish to cite from it.

Published version

HUDSPITH, Lewis, SHMAM, Faraj, DALTON, Caroline F, PRINCIVALLE, Alessandra and TUREGA, Simon (2019). Neurotransmitter selection by monoamine oxidase isoforms, dissected in terms of functional groups by mixed double mutant cycles. *Organic & Biomolecular Chemistry*.

Copyright and re-use policy

See <http://shura.shu.ac.uk/information.html>

Neurotransmitter selection by monoamine oxidase isoforms, dissected in terms of function groups by mixed double mutant cycles

Received 00th January 20xx,
Accepted 00th January 20xx

L. Hudspith^a, F. Shmam^a, C.F. Dalton^a, A. Princivalle^a and S. M. Turega^a

DOI: 10.1039/x0xx00000x

www.rsc.org/

Double mutant cycles were constructed using neurotransmitters and synthetic substrates that measure their selective binding to one monoamine oxidase (MAO) enzyme isoform over another as a function of structural change. This work measures a reduction in selectivity for the MAOB isoform of 3 to 9.5 kJ/mol on the addition of hydroxy functional groups to a phenethylamine scaffold. Replacement of hydroxy functional groups on the phenethylamine scaffold by hydrophobic substituents measures an increase in selectivity for MAOB of -1.1 to -6.9 kJ/mol. The strategies presented here can be applied to the development of competitive reversible inhibitors of MAO enzymes and other targets with structurally related isoforms.

Introduction

Neurotransmitters containing a phenethylamine scaffold are integral to signalling process in the central nervous system. These amines can be oxidised, decommissioning them by the monoamine oxidase (MAO) enzymes. The inhibition of these enzymes is a target for therapeutic development with the selectivity of candidate molecules for one isoform over another being a key consideration. Current drug development programs target the MAO enzymes along with transport proteins and receptors that bind the neurotransmitters decommissioned by the MAO enzymes.¹ The understanding of substrate and inhibitor binding is required for the development of effective inhibitors of these targets for the treatment of central nervous system (CNS) disorders, with focus on competitive inhibitors selective for monoamine oxidase B (MAOB) over monoamine oxidase A (MAOA). The understanding of selectivity of small molecule binding to the MAO enzymes and other neurotransmitter binding targets can be considered an important goal in the development of new selective inhibitors.²⁻⁵ The target

binding for both irreversible and reversible competitive inhibitors is the enzyme's active site where the redox cofactor flavin adenine dinucleotide (FAD) is located. MAOA and MAOB are mainly localized in the brain, with the expression of both MAO described in peripheral tissues.^{6,7}

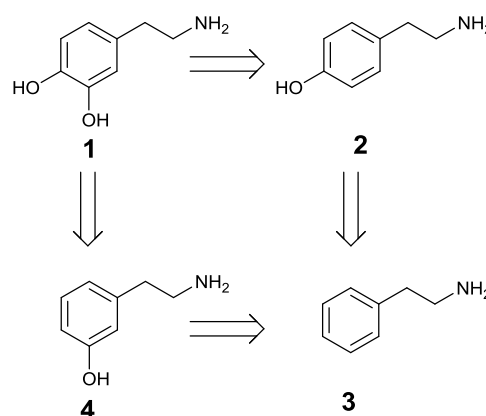


Figure 1. Theoretical dissection of dopamine, **1** to give phenethylamine, **2** via **3** or **4** through the stepwise substitution of individual functional groups.

In humans the MAO isoforms MAOA and MAOB share a 73% sequence homology, the selectivity of the MAO isoforms for endogenous neurotransmitters is provided by the size, shape and amino acid functionality of the enzymes active sites. Specifically the active site of MAOA has a volume of $\approx 550 \text{ \AA}^3$ that of MAOB $\approx 700 \text{ \AA}^3$, there are nine residues that differ between the isoforms and six residues where α -carbon positions vary more than 0.5 \AA between the isoforms.⁸ A logical step in the development of more selective inhibitors is to build a quantitative understanding of substrate recognition describing what structural changes provide the observed isoform selectivity. The molecular recognition of host-guest binding events can be quantified and rationalised at the level of individual interactions using double mutant cycles (DMCs). This strategy has been used to study the protein folding through DMCs, synthetic host-guest interaction with chemical DMCs, the effect of conformational restriction of binding affinities and the molecular recognition of supramolecular cage-guest systems.⁹⁻¹⁵ Different

^a Biomolecular Sciences Research Centre, Sheffield Hallam University, Howard Street, Sheffield, S1 1WB

† Footnotes relating to the title and/or authors should appear here.

Electronic Supplementary Information (ESI) available: [details of any supplementary information available should be included here]. See DOI: 10.1039/x0xx00000x

functional groups around a neurotransmitter substrate or inhibitor scaffold result in contributions from the resulting non-covalent interactions or lack interaction of different magnitudes to the overall binding event.¹⁶

Results and discussion

This work reports mixed double mutant cycles which, through structural changes in enzyme MAOB to MAOA and structural changes in substrate, substitution of functional groups around the ring of a phenethylamine scaffold produce DMCs that dissect the differing molecular recognition afforded by the MAO isoforms active sites. Parallels can be drawn between the reversible binding of a neurotransmitter substrate and the binding of a competitive inhibitor to an MAO isoform's active site (Figure S1). The understanding of how changes in substrate structure affect isoform selectivity can be transposed onto the design and subsequent improvement in selectivity of small molecule inhibitors for these targets.

Table 1. Michaelis-Menten parameters for compounds 1-7 measured 310 K with both MAOA and MAOB.

Substrate	MAOA		MAOB	
	$K_s / \mu\text{M}$	$k_{cat} / \text{min}^{-1}$	$K_s / \mu\text{M}$	$k_{cat} / \text{min}^{-1}$
1	260 ±10	0.40 ±0.12	400 ±100	0.11 ± 0.036
2	1600 ±50	0.29 ±0.02	1600 ±80	0.066 ±0.006
3	2300 ±6	5.6 ±1.2	54 ±4	0.048 ±0.04
4	490 ±20	0.84 ±0.12	230 ±50	0.72 ±0.12
5	45 ±3	0.54 ±0.12	29 ±2	10 ±1
6	300 ±20	0.78 ±0.18	15 ±3	14 ±6
7	69 ±4	2.3 ±0.6	7.7 ±2	33 ±1

To understand the selectivity of these neurotransmitters for one isoform over another the dissection of dopamine 1 was visualised one substitution at a time to give its phenethylamine 3 neurotransmitter core, through the tyramine 2 substrate and 3-(2-aminoethyl)phenol 4 shown in figure 1. This involves replacing the *para* and *meta* hydrogens of the phenyl ring in phenylethylamine 3 with a hydroxy functional group to give the di-substituted ring of 2 or 4 after a single substitution; a further substitution to add a second hydroxy group gives the target dopamine, 1. In the step wise substitution of phenylethylamine 3 to give dopamine 1 the size and polarity of the substrate is increased specifically by two hydroxy functional groups comprising of an oxygen hydrogen bond acceptor and a hydrogen bond donor. Dopamine 1 is a key neurotransmitter in the CNS, tyramine 2 promotes the release of monoamine release from presynaptic neurons, phenethylamine 3 acts as a stimulant or neuromodulator in the CNS of humans.¹⁷

The ethylamine functionality in these neurotransmitters is catalytically oxidised by the MAO to the corresponding acetaldehyde producing a stoichiometric equivalent of hydrogen peroxide that can be observed in real time producing kinetic data with an Amplex Red™ enzyme coupled fluorescent assay. For substrates that show a good fit to Michaelis–Menten enzyme kinetics the substrate binding constant (K_s) measures the substrate

affinity for the MAO active site, equation (1). Michaelis-Menten data sets were collected for substrates 1 to 7 with both MAOA and MAOB to allow the construction of DMCs (figure 2) through the variation of substituents R1 and R2 to dissect the substrate molecular recognition shown in figure 1. The concentration of hydrogen peroxide formation in the reactions was converted to molar values using an Amplex Red™ standard curve and plotted as a function of time, the linear portions of these reaction profiles were fit to a straight line to give a v_0 value. The Michaelis Menten curves produced from these data sets were fitted to equation (1) using nonlinear regression to give K_s and k_{cat} parameters, Table 1. The K_s values range from 45-2300 μM for MAOA and 7.7-1600 μM for MAOB, these values are used in DMC calculations, k_{cat} values are within the range expected. Recent approvals of "Xadago"(safinamide) a competitive (non-covalent) reversible MAOB inhibitor and much development of trend small molecule inhibitors for MAOB focuses on competitive (non-covalent) reversible MAO inhibitors. In this work to further develop that direction, the analysis developed focuses on the molecular recognition of the reversible substrate binding step (Figure S1), the K_s and corresponding free energy of substrate binding (ΔG_s) binding terms (Table S1).

$$v = [E]_0[S]k_{cat} / K_s + [S] \quad (1)$$

DMC method: phenylethylamine 3 to tyramine 2. The first DMC needed to investigate the structural changes in figure 1 is the substitution of the *para*-hydrogen in phenylethylamine 3 by a *para*-hydroxy to give tyramine 2, using equation (2). The step wise DMC in figure 3 shows the free energy change ($\Delta\Delta G$) for each single mutation that makes up the whole cycle. For each mutation of the cycle a single mutant $\Delta\Delta G$ is calculated by subtracting the ΔG for the product complex from the ΔG of the starting complex, following the direction of the arrows in figure 3. The single mutant **MAOB•R2** to **MAOA•R2** changing the enzyme MAOB to MAOA with the same substrate gives the difference in substrate binding of tyramine 2 between MAOB and MAOA as a negligible change -0.1 kJ/mol, the single mutant **MAOB•R1** to **MAOA•R1** difference between substrate binding of phenylethylamine 3 between the MAOB and MAOA is a favourable -9.5 kJ/mol. When the single mutant **MAOB•R2** to **MAOB•R1** changes the substrate for the same enzyme adding a *para*-hydroxy to phenylethylamine 3 to give tyramine 2 with MAOB this gives an unfavourable change in substrate binding of 8.6 kJ/mol the same single mutant **MAOA•R2** to **MAOA•R1** change with MAOA gives a small favourable change in binding of -0.9 kJ/mol. Subtracting the $\Delta\Delta G$ values for parallel mutations of the DMC (equation (2)) gives the change in selectivity for MAOB as a function of functional group substitution, meaning the addition to the phenylethylamine 3 scaffold of a *para*-hydroxy makes the tyramine 2 substrate bind 9.5 ±0.6 kJ/mol with lower affinity to MAOB relative to MAOA.

$$\Delta\Delta G = \Delta G_{\text{MAOA}\cdot\text{R1}} - \Delta G_{\text{MAOB}\cdot\text{R2}} - \Delta G_{\text{MAOA}\cdot\text{R1}} + \Delta G_{\text{MAOB}\cdot\text{R2}} \quad (2)$$

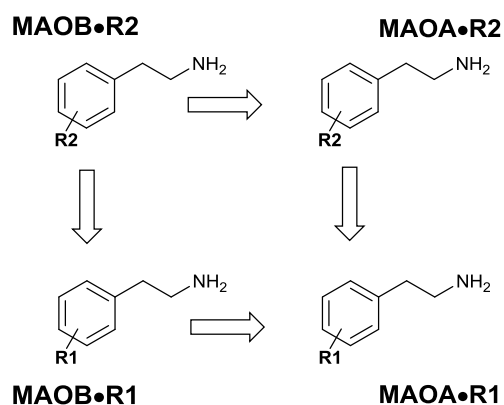


Figure 2. Theoretical dissection of dopamine, **1** to give phenethylamine, **2** via **3** or **4** through the stepwise substitution of individual functional groups.

Table 2. Measured $\Delta\Delta G$ for the DMC in fig. 3 that dissect the molecular recognition of dopamine **1** in a series of stepwise substitutions, measured at 310K.

	R1	R2	$\Delta\Delta G /$ kJ/mol	
1	<i>m</i> -OH, <i>p</i> -OH	7	<i>m</i> -Me, <i>p</i> -Me	-6.9 ± 0.9
2	<i>m</i> -H, <i>p</i> -OH	1	<i>m</i> -OH, <i>p</i> -OH	1.2 ± 0.7
2	<i>m</i> -H, <i>p</i> -OH	5	<i>m</i> -H, <i>p</i> -Me	-1.1 ± 0.2
3	<i>m</i> -H, <i>p</i> -H	2	<i>m</i> -H, <i>p</i> -OH	9.5 ± 0.6
3	<i>m</i> -H, <i>p</i> -H	4	<i>m</i> -OH, <i>p</i> -H	7.7 ± 0.8
4	<i>m</i> -OH, <i>p</i> -H	1	<i>m</i> -OH, <i>p</i> -OH	3.0 ± 0.9
4	<i>m</i> -OH, <i>p</i> -H	6	<i>m</i> -OMe, <i>p</i> -H	-5.7 ± 0.6
5	<i>m</i> -H, <i>p</i> -Me	7	<i>m</i> -OH, <i>p</i> -OH	-4.5 ± 0.6

Stepwise dissection of dopamine by DMC: phenylethylamine **3 to dopamine **1**.** The seven substrates, three endogenous and four synthetic are required for the functional group substitutions that describe the dissection of dopamine **1** to give phenylethylamine **3** using the eight DMCs shown in figure 4(a). The $\Delta\Delta G$ values for the DMC required are calculated using equation (2) and presented in Table 2. To investigate the addition of hydroxy groups to the phenylethylamine **3** scaffold four DMCs are constructed **3** to **2**, **3** to **4**, **2** to **1** and **4** to **1**. The DMCs describing the substitution of *para* or *meta* positions on the phenylethylamine **3** scaffold for hydroxy groups to give tyramine **2** or 3-(2-aminoethyl)phenol **4** give a reduction in selectivity for MAOB of 9.5 and 7.7 kJ/mol respectively. The DMCs describing the substitution of the remaining *meta* or *para* substituent on tyramine **2** or 3-(2-aminoethyl)phenol **4** for a second hydroxy group to give dopamine **1** gives a further small reduction in selectivity for MAOB of 1.2 and 3.0 kJ/mol. This shows a progressive decrease in selectivity for MAOB as two hydrogens around the aromatic ring are replaced with larger and more polar hydroxy functional groups. To investigate the role of the hydrogen bond donors in tyramine **2**, 3-(2-aminoethyl)phenol **4** and dopamine **1** analogues that no longer have the hydrogen bond donor of the hydroxy substituent; 2-(*p*-tolyl)ethan-1-amine **5**, 2-(3-methoxyphenyl)ethan-1-amine **6** and 2-(3,4-dimethylphenyl)ethan-1-amine **7** were used to build the three three DMCs **2** to **5**, **4** to **6** and **1** to **7** in Figure 2. The DMCs built from substituting the *para*-hydroxy of tyramine **2** for a *para*-methyl to give 2-(*p*-tolyl)ethan-1-amine **5** makes the substrate -1.1 kJ/mol slightly more selective for MAOB. An overview of the data in figure 4(a) is presented as a column graph in figure 4(b) to aid the visualisation of continuum of data presented.

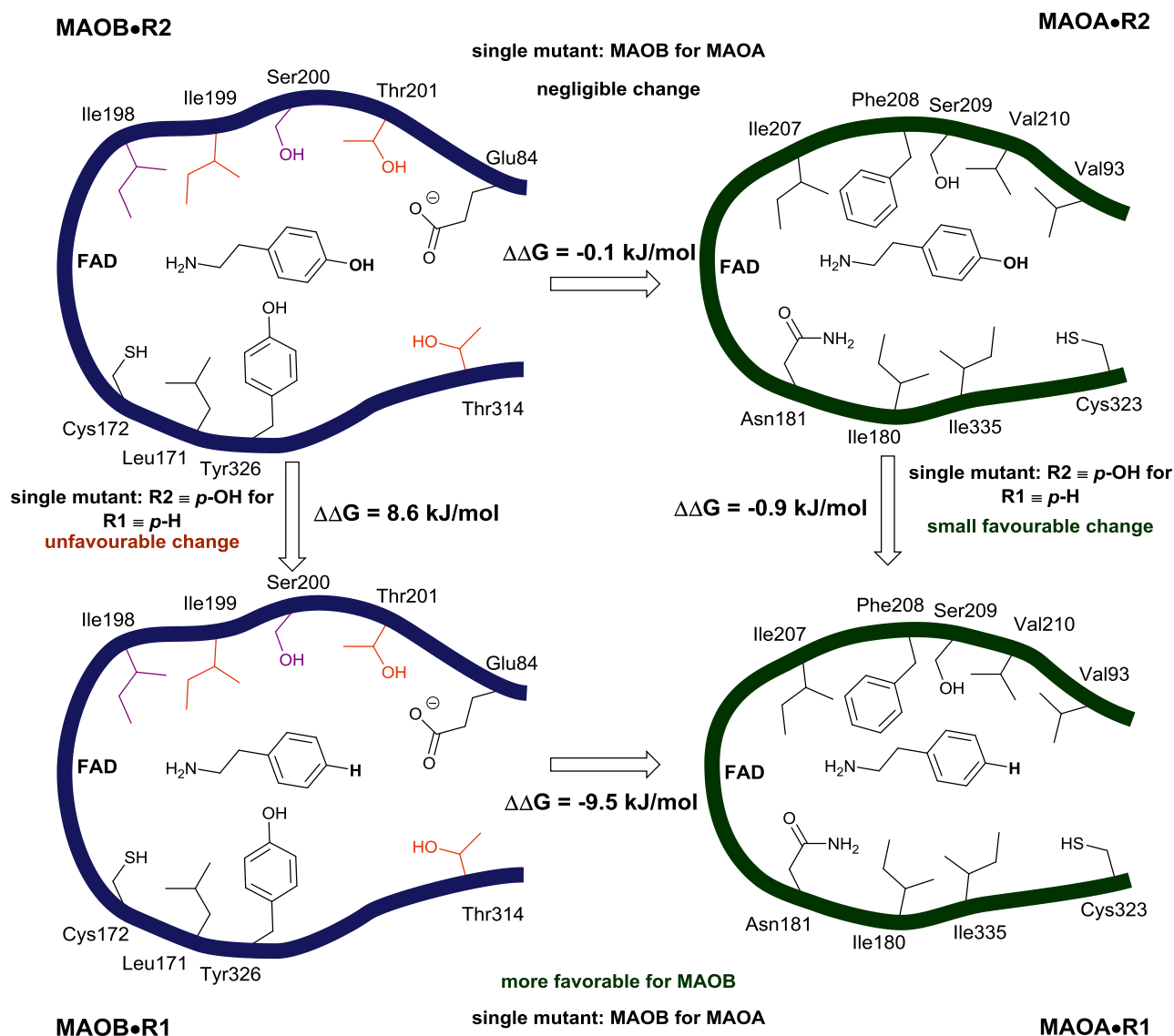


Figure 3. DMC method: phenylethylamine **3** to tyramine **2**. A mixed double mutant cycle describing the addition of a *p*-OH to phenylethylamine **3** to give tyramine **2**, built by the substitution of R2 for R1 where R1 the *p*-H in **3** is substituted with R2 the *p*-OH in **2**, with MAOA and MAOB which describing change in selectivity of binding to MAOB for this substitution. Active site residues that differ between the MAOA and MAOB are shown in black, residue positions that move more than 0.5 Å are shown in purple, residues that both differ and move more than 0.5 Å are shown in orange.

The DMCs substituting the *meta*-hydroxy of 3-(2-aminoethyl)phenol **4** for *meta*-methoxy in 2-(3-methoxyphenyl)ethan-1-amine **6** makes the substrate -5.7 kJ/mol more selective for MAOB; substituting the *para*-hydroxy and the *meta*-hydroxy of dopamine **1** for *para*-methyl and *meta*-methyl to give 2-(3,4-dimethylphenyl)ethan-1-amine **7** results in this substrate being -6.9 kJ/mol more selective for MAOB. Relating these results to the structure of the MAO active sites, an increase in hydrophobic surface area groups provides an increase in MAOB selectivity and a decrease in hydrophobic functional groups provides a decrease in selectivity for MAOB. An explanation for this observation is the increased size of the MAOB cavity compared to that of MAOA provides a decreased opportunity for favourable hydrophobic contacts between the substrate active site

The bulk treatment of substitutions changing hydrogen bond donors, hydrogen bond acceptors and hydrophobic contacts neglects the powerful selectivity of enzyme active sites. To probe this important aspect of substrate recognition the $\Delta\Delta G$ of substrate binding for the substitution of phenethylamine **3** for the individual enzymes, MAOA and MAOB is shown in Tables S2 and S3. For MAOA all substitutions of phenethylamine **3** result in an increase in substrate binding affinity but for MAOB only substitutions that lack a hydrogen donor result in an increase in substrate binding affinity, substitutions that involve the addition of a hydrogen bond acceptor result in a reduction in substrate binding.

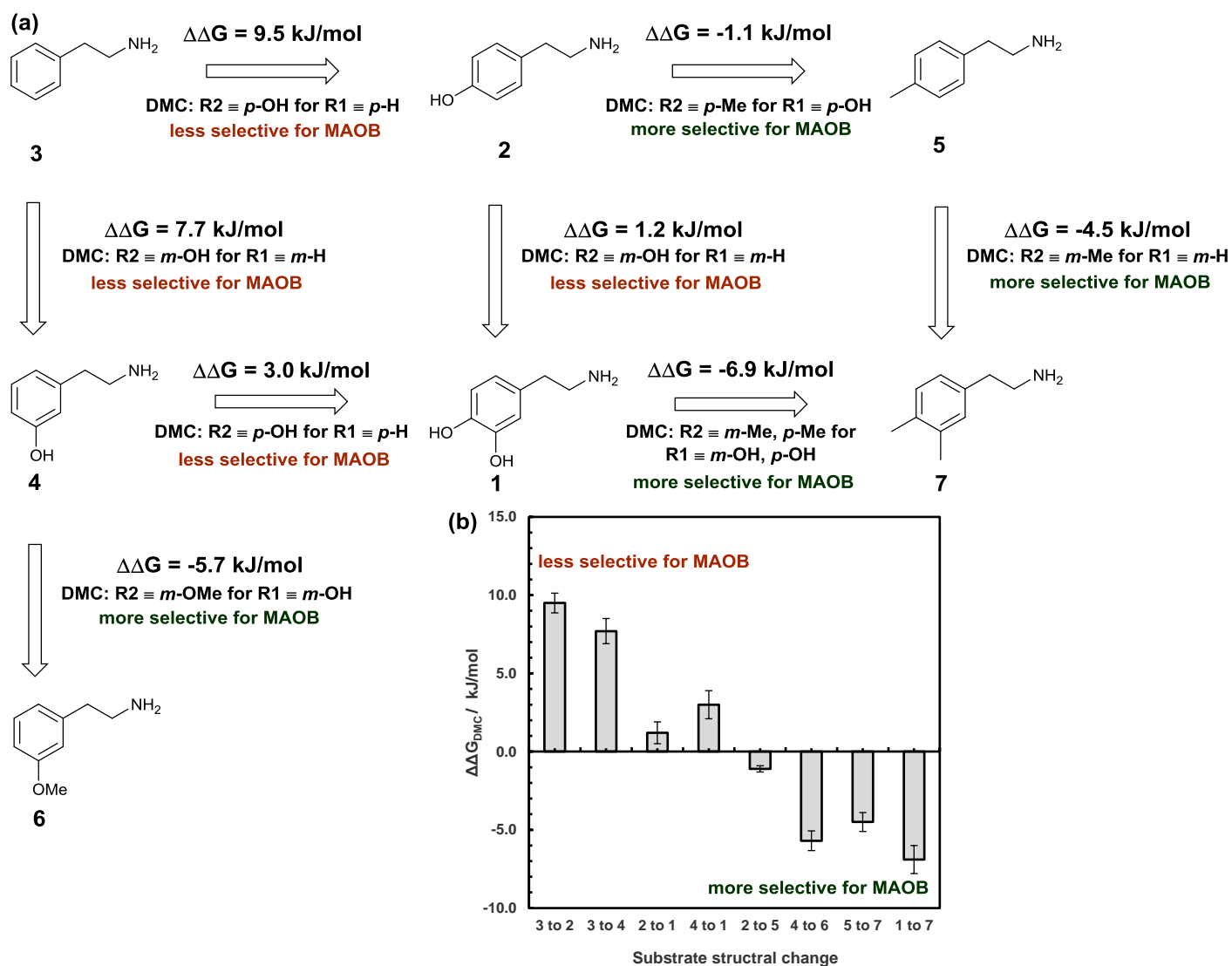


Figure 4. (a) Stepwise dissection of dopamine by DMC: phenylethylamine **3** to dopamine **1**. Values of $\Delta\Delta G$ at 310 K for DMCs that describe the change in selectivity for MAOB over MAOA for the substitution of the *p*-H and *m*-H of phenylethylamine **3** for hydroxy groups to give substrates **1, 2**, and **4**; using the $\Delta\Delta G$ values for **3** to **2**, **2** to **5**, **4** to **1** and **2** to **1**. For the loss of hydrogen bond donors values of $\Delta\Delta G$ at 310 K for DMCs that describe the change in selectivity for MAOB over MAOA for loss of hydroxy groups to give substrates **5**, **6** and **7**; using the $\Delta\Delta G$ values for **2** to **5**, **5** to **7**, **1** to **7** and **4** to **6**. (b) Data from Stepwise dissection of dopamine by DMC: phenylethylamine **3** to dopamine **1** represented as a column graph.

Structural data for competitive (non-covalent) reversible inhibitors bound to MAOA and MAOB as host-guest complexes was retrieved from the protein data bank, the reversible inhibitors bind to the MAO active site through hydrogen bonds to the FAD cofactor, ring to carbonyl π -stacking, hydrophobic contacts, hydrogen bond from

active site residues to the bound inhibitor and hydrogen bonds from the bound inhibitor to ordered active site waters.¹⁸⁻²⁰ Increasing the hydrophobic surface area of substrates can increase the opportunity for hydrophobic contacts and the displacement of cavity waters increasing the magnitude of the hydrophobic

contribution to the binding.²¹⁻²³ Addition of specific hydrogen bonds between inhibitors and enzyme active sites confers stability to the enzyme substrate complex; here we demonstrate that the addition of hydrogen bond donors reduces the strength of substrate binding to MAOB. Substitution of a hydrogen bond donor containing functionality for one without the hydrogen bond donor makes a substrate more selective for MAOB. To rationalise these observations we use the GOLD docking software to generate binding poses of the substrates to the active sites of the MAOA and MAOB enzymes. This was achieved using crystal structures of MAOA (PDB code: 2Z5X) and MAOB (PDB code: 3PO7) containing small competitive (non-covalent) reversible inhibitors in the active site. The docking studies produced favourable binding conformations for MAOB with substrates **1**, **2** and **4** that contained a hydrogen bond between the amide carbonyl of Ile-199 and a substrate hydroxy group. In MAOA the Ile-199 residue is mutated to Phe208 again favourable binding conformations hydrogen bonds between the hydroxy groups of **1**, **2** and **4** and the Phe208 residue were observed Figure 2 and Figure S1. As both active sites have the capacity to form similar hydrogen bonds to the substrates it is possible to consider that the behaviours observed are due to a reduction in hydrophobic surface area upon a substitution of a hydrogen atom for a polar hydroxy group and the effect this has on hydrophobic contacts between a larger MAOB and smaller MAOA active site cavity.

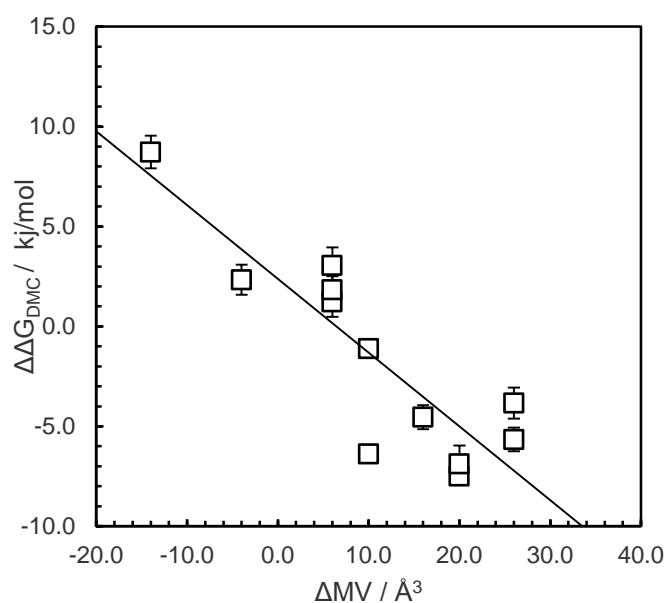


Figure 5, The plot of change in molecular volume ($\Delta MV / \text{\AA}^3$) against $\Delta \Delta G$ for the DMC in built from all possible combinations of single and double functional group substitutions using substrates **1** to **7**, the linear trend line has $R^2 = 0.763$.

To further understand the balance between polar hydrogen bond donors and hydrophobic substituents a further nine DMC were built from all possible combinations of single and double functional group substitutions using substrates **2** to **7** to investigate the substitution of polar substituents for none polar substituents. The $\Delta \Delta G$ for these 15 cycles that describe the substitution of polar

substituents for non-polar substituents can be plotted against the structural parameters, change in; molecular volume, surface area and total polar surface area (TPSA) figures 5, S3 and S4 respectively. The plot that demonstrate the best correlation is figures 5, change in molecular volume, can be related to exclusion of waters and increased hydrophobic contacts, there is a trend for an increase in MAOB selectivity as molecular volume increases. The larger the change in; molecular volume or surface area the larger the increase selectivity for MAOB, making this a useful structural parameter for use in considering the selection of functional groups for substitution in and addition to an inhibitor scaffold. Variance in these plots is likely due to mismatches between the structures of the substrates and the enzyme active site, this can be explored as the number of examples is increased in future work. There is a less strong correlation between surface area or ΔTPSA and selectivity for MAOB figure S3 and S4.

Conclusion

The DMC constructed in this work describe the specific substitutions of single and double function groups around a phenethylamine scaffold, DMC have been constructed in order to calculate the change in selectivity of substrate binding for MAOB over MAOA as a result of these substitutions. Seven substrates have been used to dissect the molecular recognition of the key neurotransmitter dopamine **1**; these include both endogenous and synthetic substrates for the MAO enzymes. These cycles have been used to build up a molecular recognition profile for dopamine **1** probing the free energy-structure profiles for increasing substrate surface area and number of hydrogen bond donors. This suggests a relationship between the amount of hydrophobic contacts in the substrate-enzyme complex and free energy of substrate binding as demonstrated previously by synthetic ligand-receptor studies in water.²⁴ The DMC approach and data presented here can be applied to achieve this structural changes have to occur that result in a molecular recognition interface that is made up of multiple weak interactions. Through the inclusion of additional weak interactions and the optimisation of the efficiency with which each of the weak interactions is made the affinity of the inhibitor for the active site can be increased.^{25, 26} The effect of adding functional groups that form additional weak interactions and structural changes to functional group that already make interactions can be quantified using this DMC approach. Initial results suggest that addition of bulky and hydrophobic substituents can be used to make inhibitors more selective for MAOB the effect of this on a substituted inhibitor scaffold can be quantified through the construction of further DMCs. The data collected will expand data sets that allow the determination of general trends and correlations that can influence further development. To utilise the data sets collected and address selectivity in a predictive way the data points collected can be used to build a training set for a linked theoretical approach using a bespoke scoring function for docking software this approach can be used as a powerful predictive tool for the virtual screening of large compound libraries containing accessible functional group substitutions for the effect on isoform selectivity.²⁷ Considering that many biological macromolecules (in addition to MAOA and MAOB) that bind monoamine neurotransmitters are

current drug targets this physical-organic chemistry approach can be transferred to further targets with structurally related isoforms, relevant to medicinal chemistry and elucidation of biological mechanisms.²⁸ This will provide an understanding of the effects of structural changes on isoform selectivity allowing the development of more selective molecules.

Experimental

a full description of experimental work is included in the supporting information.

Conflicts of interest

There are no conflicts to declare.

Notes and references

- 1 A. Bach, N. Lan, D. Johnson, C. Abell, M. Bembenek, S. Kwan, P. Seeburg and J. Shih, *P.N.A.S. U.S.A.*, 1988, **85**, 4934-4938
- 2 B. Kumar, Sheetal, A. K. Mantha and V. Kumar, *RSC Adv.*, 2016, **6**, 42660
- 3 L. M. Scorr and S. A. Factor, *J. Neurol. Sci.*, 2018, **389**, 43-47
- 4 D. S. Goldstein, I. J. Kopin and Y. Sharabi, *Pharmacol. Ther.*, 2014, **144**, 268-282;
- 5 M. Costas-Lago, P. Besada, F. Rodríguez-Enríquez, D. Viña, S. Vilar, E. Uriarte, F. Borges and C. Terán, *Eur. J. Med. Chem.*, 2017, **139**, 1-11
- 6 L. W. Thorpe, K. N. Westlund, L. M. Kochersperger, C. W. Abell and R. M. Denney, *J. Histochem. Cytochem.*, 1987, **35**, 23-32
- 7 J. Schneider, C. H. Markham, *Exp. Neurol.*, 1987, **97**, 465.
- 8 L. De Colibus, M. Li, C. Binda and A. Lustig, *P.N.A.S. U. S. A.*, 2005, **102**, 12684-12689
- 9 G. Schreiber and A. R. Fersht, *J. Mol. Bio.*, 1995, **248**, 478.
- 10 C. A. Hunter, M. C. Misuraca and S. M. Turega, *J. Am. Chem. Soc.*, 2011, **133**, 582
- 11 W. Jiang, K. Nowosinski, N. Löw L., E. V. Dzyuba, F. Klautzsch, A. Schäfer, J. Huuskonen, K. Rissanen and C. A. Schalley, *J. Am. Chem. Soc.*, 2012, **134**, 1860
- 12 M. Whitehead, S. Turega, A. Stephenson, C. A. Hunter and M. D. Ward, *Chem.Sci.*, 2013, **4**, 2744
- 13 S. Henkel, M. C. Misuraca, Y. Ding, M. Guitet and C. A. Hunter, *J. Am. Chem. Soc.*, 2017, **139**, 6675
- 14 S. L. Cockroft and C. A. Hunter, *Chem. Soc. Rev.*, 2007, **36**, 172-188.
- 15 H. Adams, E. Chekmeneva, C. A. Hunter, M. C. Misuraca, C. Navarro and S. M. Turega, *J. Am. Chem. Soc.*, 2013, **135**, 1853-1863.
- 16 C. Hunter and H. Anderson, *Angew. Chem Int. Ed.*, 2009, **48**, 7488-7499
- 17 B. Borowsky, N. Adham, K. Jones, R. Raddatz, R. Artymyshyn, K. Ogozalek, M. Durkin, P. Lakhani, J. Bonini, S. Pathirana, N. Boyle, X. Pu, E. Kouranova, H. Lichtblau, F. Ochoa, T. Brancheck and C. Gerald, *P.N.A.S. U.S.A.*, 2001, **98**, 8966-8971
- 18 S. Son, J. Mat, Y. Kondou, M. Yoshimura, E. Yamashita and T. Tsukihara, *P.N.A.S. U.S.A.*, 2008, **105**, 5739.
- 19 C. Binda, M. Aldeco, A. Mattevi and D. E. Edmondson, *J. Med. Chem.*, 2011, **54**, 909
- 20 A. Maršavelski and R. Vianello, *Chem. Eur. J.*, 2017, **23**, 2915-2925
- 21 P. W. Snyder, J. Mecinovic, D. T. Moustakas, Thomas, Samuel W., I., II, M. Harder, E. T. Mack, M. R. Lockett, A. Heroux, W. Sherman and G. M. Whitesides, *P.N.A.S. U.S.A.*, 2011, **108**, 17889
- 22 A. J. Metherell, W. Cullen, N. H. Williams and M. D. Ward, *Chem. Eur. J.*, 2018, **24**, 1554-1560
- 23 J. Cramer, S. G. Krimmer, A. Heine and G. Klebe, *J. Med. Chem.*, 2017, **60**, 5791-5799.
- 24 S. Turega, W. Cullen, M. Whitehead, C. A. Hunter and M. D. Ward, *J. Am. Chem. Soc.*, 2014, **136**, 8475-8483.
- 25 K. N. Houk, A. G. Leach, S. P. Kim and X. Zhang, *Angew. Chem Int. Ed.*, 2003, **42**, 4872-4897
- 26 P. Groves, M. S. Searle, M. S. Westwell and D. H. Williams, *J. Chem. Soc., Chem. Comm.*, 1994, 1519-1520.
- 27 C. A. Hunter and S. Tomas, *Chem. Biol.*, 2003, **10**, 1023-1032.
- 28 W. Cullen, S. Turega, C. A. Hunter and M. D. Ward, *Chem. Sci.*, 2015, **6**, 2790-2794
- 29 S. J. Pike, J. J. Hutchinson, C. A. Hunter, *J. Am. Chem. Soc.* **2017**, **139**, 6700